

Kink-antikink vortex transfer in periodic-plus-random pinning potential: Theoretical analysis and numerical experiments

W. V. Pogosov^{1,2}, H. J. Zhao¹, V. R. Misko¹, and F. M. Peeters¹

¹*Departement Fysica, Universiteit Antwerpen, Groenenborgerlaan 171, B-2020 Antwerpen, Belgium and*

²*Institute for Theoretical and Applied Electrodynamics,*

Russian Academy of Sciences, Izhorskaya 13, 125412, Moscow, Russia

(Dated: December 1, 2018)

The influence of random pinning on the vortex dynamics in a periodic square potential under an external drive is investigated. Using theoretical approach and numerical experiments, we found several dynamical phases of vortex motion that are different from the ones for a regular pinning potential. Vortex transfer is controlled by kinks and antikinks, which either preexist in the system or appear spontaneously in pairs and then propagate in groups. When kinks and antikinks collide, they annihilate.

PACS numbers: 74.25.Qt

The behavior of an elastic media under the competitive action of a regular potential and disorder is a common problem in various fields of modern physics. Examples of such media are vortex lattices in superconductors^{1,2,3,4} or in Bose-Einstein condensates of ultracold atoms⁵, interacting colloids on periodic substrates^{6,7}, charge and spin density waves in metals⁸, polarization density waves in ferroelectrics and many others. Regular pinning potential can be either of artificial origin, as in nanostructured superconductors and in Bose-Einstein condensates with optical lattices, or it can be imposed by the crystal structure of the material. In superconductors, pinning efficiency determines the value of the critical current which is of great practical importance. Theoretical description of such systems is a quite complicated problem, which in one-dimensional case can be reduced to the well-known Frenkel-Kontorova model^{8,9}.

Recently, two-dimensional lattice of repelling particles in the presence of square pinning potential and disorder was investigated theoretically and numerically¹⁰. In the case of weak disorder, a pinned vortex lattice is disturbed by specific defects consisting of elastic strings of depinned vortices. It was found that these strings are able to intersect and form branched fractal-like clusters, which can percolate through the system. The aim of the present letter is to investigate the vortex dynamics in such a system and look for correlations between the static defects and the dynamical phases under an external drive.

Model.— We model a three-dimensional (3D) superconducting slab by a 2D simulation cell assuming the vortex lines are parallel to the cell edges^{2,3}, in the presence of a regular square array of pinning sites with period a and randomly distributed pins of comparable concentration. Pinning potential, produced by a single site, is modeled by a parabolic function, with U_{reg} (U_{ran}) and σ_{reg} (σ_{ran}) being the depth and size of potential wells of regular (random) origin; $\sigma_{reg}, \sigma_{ran} \ll a$ and $\sigma_{ran} \sim \sigma_{reg}$. We will focus mostly on the weak-disorder regime, i.e., when the maximum pinning force by one regular site, $f_{reg} = 2U_{reg}/\sigma_{reg}$, is significantly larger than that for a random site, $f_{ran} = 2U_{ran}/\sigma_{ran}$. Vortices are treated

within the London approximation (i.e., as point-like particles). We consider the case of the first matching field, i.e., when the number of vortices is equal to the number of regular pins. To study the motion of vortices, we use molecular-dynamics simulations, and we numerically integrate the overdamped equations of motion^{2,3}:

$$\eta \mathbf{v}_i = \mathbf{f}_i = \mathbf{f}_i^{vv} + \mathbf{f}_i^{vp} + \mathbf{f}^d + \mathbf{f}_i^T. \quad (1)$$

Here, \mathbf{f}_i is the total force acting on vortex i ; \mathbf{f}_i^{vv} and \mathbf{f}_i^{vp} are the forces due to the vortex-vortex and vortex-pin interactions, respectively; \mathbf{f}^d is an external driving force (i.e., a Lorentz force created by an applied current); \mathbf{f}_i^T is the thermal stochastic force. A simulation cell contains 20×20 regular pins, and we use periodic boundary conditions to simulate an infinite array. To explain the results of numerical experiments, we also use an analytical approach: in various situations most of the vortices remain pinned, so that the vortex transfer occurs through collective defects, which can be described reasonably well by just few parameters and by using assumptions of elasticity theory. Below we will present our results for the following set of parameters: $a = \lambda(T)$, $\sigma_{reg} = 0.15a$, $\sigma_{ran} = 0.2a$, $f_{reg} = 0.6f_0$, where $f_0 = \Phi_0^2/32\pi^2\lambda(T)^3$, numbers of regular and random sites being the same.

Depinning of stripes (phase I).— Very weak driving results in no vortex motion (pinned regime). If the driving force F_d reaches some threshold value $F_d^{(I)}$, part of vortices start to move. The vortex motion is not individual, since vortices travel collectively in a soliton-like manner, being localized within vortex rows. Moving collective structures are just depinned stripe-like defects, which were predicted in the static configurations¹⁰. Each defect contains either one extra vortex (kink) or one vacancy (antikink). Kinks propagate in the direction of an applied force, so that they are solitary compression waves of vortex row, as seen from Fig. 1 which shows kink motion. Vacancy-based antikinks flow in the opposite direction; they can be considered as decompression waves. The number of vortices D in a static stripe depends on the balance between the vortex-vortex interaction energy

and the energy gained due to the displacement of vortices from the centers of regular pins

$$D \approx \left\{ \frac{a}{\lambda(T)} \frac{(\Phi_0/2\pi\lambda(T))^2}{2(U_{reg} - U_{reg}^{hp})} K_1[a/\lambda(T)] \right\}^{1/2}, \quad (2)$$

where U_{reg}^{hp} is the critical U_{reg} , below which the inter-vortex interaction dominates over the regular pinning, so that it becomes energetically favorable for the vortex lattice to switch globally from the square configuration to the so-called half-pinned phase^{10,11}. In this phase, vortices in odd rows remain pinned, while vortices in even rows are shifted with respect to them over $a/2$, the periodicity of the lattice being preserved. Eq. (2) implies that when approaching U_{reg}^{hp} , the stripe becomes infinitely long. For long stripe, i.e., $D \gg 1$, we found the criterion for the instability of the pinned stripe, in leading order in $1/D$. The threshold occurs, when the *total* driving for D vortices in the stripe becomes equal to the resistance force produced by the first pinned vortex in front of the stripe, which prevents its motion, and the last pinned vortex behind the stripe,

$$F_d^{(I)} \approx \frac{2f_{reg}}{D}. \quad (3)$$

Eq. (3) demonstrates that the stripe behaves nearly as a *rigid* body containing D particles and this is the explanation why it is depinned at relatively low driving force, $F_d^{(I)} \ll f_{reg}$. Fig. 2 presents typical numerically calculated average vortex velocity, after steady flow is achieved, as a function of driving, where one can clearly see distinct dynamical regions for a weakly disordered regime, while for the stronger disorder case they are smeared out due to chaotization. Note that in the particular initial configuration for $f_{rand} = f_{reg}/6$ there was no stripe in the simulation region, which is reflected by the absence of any current up to the dynamical phase II (curve 1 in Fig. 2). The results of Eqs. (2) and (3) are in good agreement with our numerical simulations: depinning of stripes is predicted to occur at $F_d^{(I)} \approx 0.28$ ($D \approx 5$, as calculated from Eq. (2)), while in the numerical simulations this value is around 0.23 at $f_{rand} = f_{reg}/3$.

Kinks and antikinks can collide and *annihilate*. Another remarkable but quite rare process in the weak disorder regime process is soliton sticking by bunches of random pins. These two processes lead to a decay of the total current in time. Fig. 3 shows typical time dependences of the current, where two examples are addressed, when kinks and antikinks annihilate (curve 1) and when they persist (curve 1'). It is obvious, however, that in infinite systems all the kinks and antikinks have to disappear, since the total number of kinks and antikinks in a single row is the same. Nonvanishing motion in the weak disorder regime thus appears as an artifact of a finite-size simulation cell with periodic boundary conditions.

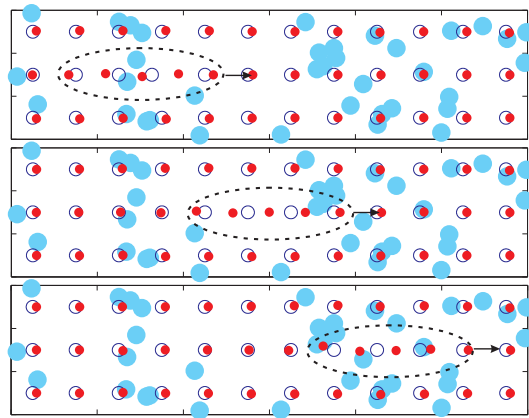


FIG. 1: (Color online) Motion of the stripe shown by three snapshots. Irregular blue (light gray) spots represent positions of random pins, red (dark gray) filled circles show positions of vortices, and regular black open circles correspond to periodic pins. Dashed lines are guides to the eye indicating positions of defects, and arrows show the direction of their motion.

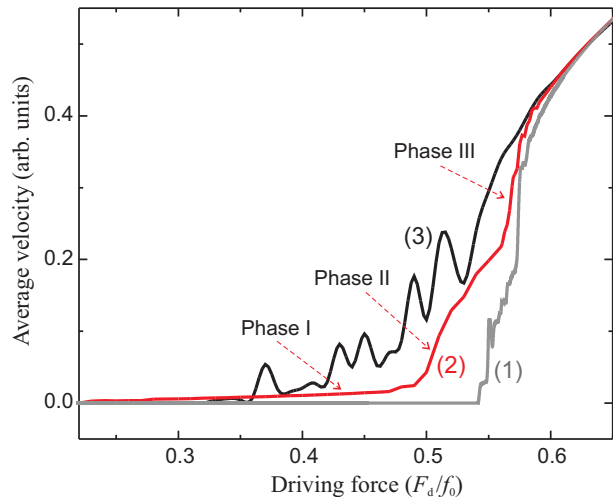


FIG. 2: (Color online) The average vortex velocity as a function of driving for different values of the random pinning force: $f_{rand} = f_{reg}/6$ (curve 1), $f_{rand} = f_{reg}/3$ (2), $f_{rand} = f_{reg}/2$ (3).

Note that static defects in the weak and intermediate disorder regime consist not only of stripes. Stripes can be just parts of clusters, some of which are large and branched¹⁰. Naively one may expect that these clusters act as easy-channels for vortex transfer. Instead, we found that low driving partially heals defects. The reason is that clusters basically consist of two types of segments¹⁰: Segments of the first kind contain no vacancies or excess vortices, in contrast with segments of the second type, which are nothing but stripe-like defects. For low driving, vortices inside segments of the first kind move collectively to their nearest vacant pins. Such a delicate healing, however, is not possible for segments of the second type. Therefore, stripes do persist in the sample and very low driving leads to fragmentation of clusters. A typical driving force, which heals such defects, can be

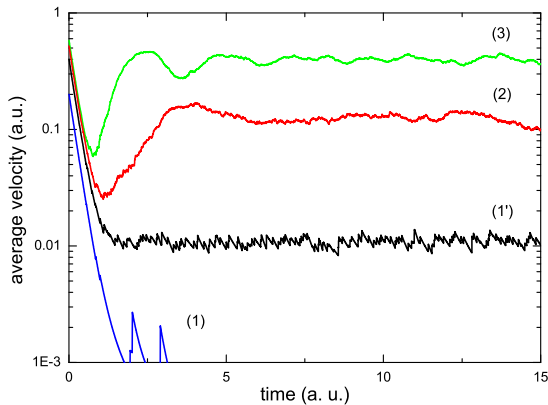


FIG. 3: (Color online) Time dependence of the average vortex velocity for different dynamical phases at $f_{rand} = 0.2$. Here $t_0 = 4\pi^2\lambda(T)^4\eta/\Phi_0^2$. Curves 1 and 1' correspond to phase I at $F_d = 0.4$ and 0.2 , respectively. Curves 2 and 3 show phases II and III for $F_d = 0.52$ and 0.57 , respectively.

estimated by considering an infinite chain of depinned vortices. An effective pinning force for vortices from the chain is created by interactions with surrounding rows of pinned vortices¹⁰. By performing a summation in reciprocal space, we obtain the following estimate:

$$F_d^{(heal)} \approx \frac{\Phi_0^2}{2\pi^2\lambda(T)^2a} e^{-2\pi}. \quad (4)$$

In the relevant range of parameters, $F_d^{(heal)} \ll F_d^{(I)}$.

Generation of kink-antikink pairs (phase II).— When driving approaches certain critical value $F_d^{(II)}$, kink-antikink pairs are created spontaneously. New kinks move in the direction of the drive, whereas antikinks propagate in the opposite direction. The corresponding dynamical phase is presented in Fig. 2 by a cusp in curves 1 and 2. Because of the intensive generation of new kinks and antikinks, average current increases significantly compared to the first dynamical phase, as seen from Fig. 3. Most of the pair generation events are triggered by moving stripes in adjacent rows, which create an additional washboard drive due to vortex-vortex repulsion. Such a process is shown in Fig. 4 by three snapshots: one of the vortices is depinned, then it creates an area of vortex row compression in front of itself and the area of decompression behind, these two areas being transformed into a kink and antikink. It is easy to realize that the amplitude of the additional periodic drive is equal to $F_d^{(heal)}$ in the limit of long kinks, so the total effective driving in the row, next to the moving stripe, is $F_d^{(eff)} \approx F_d + F_d^{(heal)}$. However, a comparison with the numerical results shows that this value is too low to explain our numerical data: $F_d^{(heal)}$ is only around 0.03, while the difference between f_{reg} and $F_d^{(II)}$ is clearly disorder-dependent: it is about 0.1 for $f_{rand} = f_{reg}/3$ and 0.05 for $f_{reg}/6$ (besides, there were no preexisted kinks within a simulation region in the latter case). The analysis of vortex motion patterns reveals that kink-antikink pairs are generated not everywhere. The reason

is that there are some weak points, where vortices are additionally strongly displaced in the direction of drive by random pins. Concentration of these weak points depends on the external drive, i.e., on the displacement r_0 of vortices inside cores, $r_0 \approx \sigma_{reg}F_d^{(eff)}/f_{reg}$. Depinning then occurs, if a pinning force by a random pin is nonzero in this point, which already restricts the position of the random pin. Another condition is that the force, produced by the random pin at the edge of the regular pin, together with $F_d^{(eff)}$ must dominate the force by the regular site. From these two conditions, we found a value of the external drive, for which an appropriate position of a random pin exists

$$F_d^{(II)} \approx \frac{f_{reg} - f_{ran}(1 - \sigma_{reg}/\sigma_{ran})}{1 + (f_{ran}/f_{reg})(\sigma_{reg}/\sigma_{ran})} - F_d^{(heal)}. \quad (5)$$

Starting from $F_d = F_d^{(II)}$, a probability for the creation of kink-antikink pairs is nonzero. We found that above $F_d^{(II)}$, concentration of weak points grows as $\sim (F_d - F_d^{(II)})^{3/2}$, so that the kink-antikink pair generation intensifies. Moreover, some pairs start to nucleate spontaneously in weak points, without the assistance of moving defects (in particular, for the case of $f_{reg}/6$, when no preexisted stripes were found within the simulation region). Note that Eq. (5) was obtained under the assumption that a depinning is due to the action of a single random pin, without overlap with other ones, such overlaps being able to produce a larger total pinning force. However, events of this sort are very rare and they do not smear $F_d^{(II)}$ significantly. Also, we didn't take into account the mutual repulsion of vortices, which acts against the vortex depinning: according to our estimates, the resistance force is too small to noticeably change $F_d^{(II)}$. Eq. (5) is in a reasonably good agreement with our numerical results of Fig. 2 for weak disorder, $f_{rand} = f_{reg}/3$ and $f_{reg}/2$ (in the latter case one has to drop $F_d^{(heal)}$ from Eq. (5), since there were no preexisted stripes in our simulation region). In the limit of very weak disorder, Eq. (5) reduces to $F_d^{(II)} \approx f_{reg} - f_{ran} - F_d^{(heal)}$, which clearly shows a competition between regularity and disorder, the latter factor being enhanced by moving kinks through an additional term $F_d^{(heal)}$. We also notice that, due to a continuous generation of kink-antikink pairs, vortex transfer within phase II no longer decays in time, as in phase I. Motion occurs via groups of kinks and antikinks propagating in opposite directions and creating, from time to time, new defects, one of which joins the same group, whereas its counterpart starts to flow in the opposite direction. Pairs can also be created without the assistance of previously excited stripes. In steady flow regime, replication of defects has to be balanced with their annihilation, under collisions of individual kinks and antikinks or their groups.

Free proliferation of kink-antikink pairs (phase III).— We found third dynamical phase, which shows up as the last distinct region in curves 1 and 2 in Fig. 2. Care-

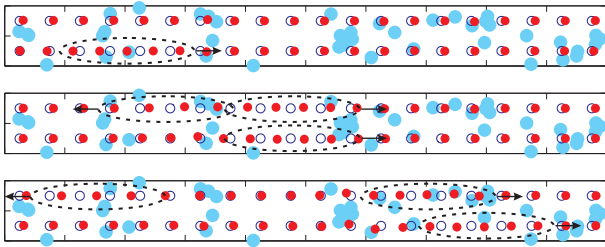


FIG. 4: (Color online) The same as Fig. 1 but with generation of kink-antikink pair by moving stripe, shown by snapshots. Initially kink flows in the bottom row, then it creates a kink-antikink pair in the upper row.

ful analysis of numerical data has indicated that, in this phase, kink-antikink pairs start to proliferate freely not only in weak points: preexisted kinks immediately generate kinks and antikinks; in their turn, these defects create new pairs, and so on. The area of vortex motion rapidly extends until it covers the whole simulation region. Mathematically, in this regime, washboard drive produced by moving kink, is already strong enough to generate kink-antikink pairs by itself. The corresponding driving is given by

$$F_d^{(III)} \approx f_{reg} - F_d^{(heal)}. \quad (6)$$

In phase III, no “islands” are found, where vortices can be pinned for a long time. According to Eq. (6), $F_d^{(III)}$ is 0.57, and this value again is in good agreement with the numerical results, shown in Fig. 2.

Let us now briefly discuss the dynamics of vortices, when the disorder is no longer very weak, so that it not only triggers motion of defects, but also significantly affects it. The general tendency is that disorder smears out well-separated dynamical phases, as seen from Fig. 2. Stripes can now easily jump from row to row and bend. However, very surprisingly, soliton-like origin of the vortex transfer is extremely robust, up to the regime of strong disorder, $f_{ran} \sim f_{reg}$. In the regime of very strong disorder, $f_{ran} \gg f_{reg}$, vortex flow is localized in narrow streams, in which vortices flow one by one. Another mechanism of vortex transfer is pumping, when vortices are pushed into some traps, until their mutual

repulsion breaks the blockade.

Note that here we analysed the first-matching-field regime, while a little imbalance between the numbers of regular pins and vortices could serve as an additional source of disorder. As was shown in Refs.^{2,3}, this imbalance results in different dynamical regimes including vortex flow in “incommensurate rows” and negative-differential-resistivity (NDR) parts of the VI-curve of N-^{2,3} and S-type³. Very recently, the first experimental observation of the N-type NDR phase has been reported¹². (See also a related experiment¹³ on a triangular array of pins, where channeling of vortices can be suppressed by the random removal of pinning sites¹⁴.)

Conclusions.— We studied the competitive effect of periodic square and weak random pinning potentials on the dynamics of vortices in two dimensions. We found new dynamical phases, which are established through a cascade of transitions. There are three phases, in which vortices move in a soliton-like collective structure travelling within individual vortex rows. These are kinks, each containing an excess vortex and moving in the direction of an external drive, and antikinks, flowing in the opposite direction and containing a vacancy. When colliding, kinks and antikinks annihilate. Initial motion is triggered by depinning of preexisted static kinks and antikinks. In the second regime, moving defects generate secondary kink-antikink pairs in adjacent rows at certain weak points, which are more corrupted by disorder. In the third regime, these pairs are freely generated by moving kinks and antikinks, i.e., without help of disorder.

Although we have concentrated on vortices in superconductors, it is clear that similar dynamical regimes will be realized in other two-dimensional systems with periodic lattice potentials, containing repelling particles. Moreover, disorder-induced kink-antikink generation under an external drive can appear as a rather universal phenomenon, which exists for systems and lattice potentials of various dimensionalities.

This work was supported by the “Odysseus” Program of Flemish government, FWO-VI, and IAP. W.V.P. acknowledges support from RFBR (contract No. 06-02-16691). V.R.M. acknowledges support from the EU MC Programme, Contract No. MIF1-CT-2006-040816.

¹ M. Baert *et al.*, Phys. Rev. Lett. **74**, 3269 (1995).

² C. Reichhardt *et al.*, Phys. Rev. Lett. **78**, 2648 (1997); Phys. Rev. B **58**, 6534 (1998).

³ V.R. Misko *et al.*, Phys. Rev. Lett. **96**, 127004 (2006); Phys. Rev. B **75**, 024509 (2007).

⁴ G.R. Berdiyrov *et al.*, Phys. Rev. B **76**, 134508 (2007).

⁵ S. Tung *et al.*, Phys. Rev. Lett. **97**, 240402 (2006).

⁶ A. Libál *et al.*, Phys. Rev. Lett. **97**, 228302 (2007).

⁷ D. Deb and H.H. von Grunberg, J. Phys.: Condens. Matter **20**, 245104 (2008).

⁸ P.M. Chaikin and T.C. Lubensky, *Principles of condensed*

matter physics, Cambridge Univ. Press, Cambridge (1995).

⁹ O. M. Braun and Y. S. Kivshar, *The Frenkel-Kotlovova Model*, Springer, Cambridge (2004).

¹⁰ W. V. Pogosov *et al.*, Phys. Rev. B **79**, 014504 (2009).

¹¹ W. V. Pogosov *et al.*, Phys. Rev. B **67**, 014532 (2003).

¹² J. Gutierrez, A.V. Silhanek, J. Van de Vondel, W. Gillijns, and V.V. Moshchalkov, unpublished.

¹³ M. Kemmler *et al.*, Phys. Rev. B **79**, 184509 (2009).

¹⁴ C. Reichhardt and C.J. Olson Reichhardt, Phys. Rev. B **76**, 094512 (2007).